Fermi liquids, and their phase transitions

From Chapter 18 of *Quantum Phase Transitions*, Second Edition Cambridge University Press

Subir Sachdev
Department of Physics, Harvard University, Cambridge MA 02138

The Fermi liquid is perhaps the most familiar quantum many-body state of solid state physics. It is the generic state of fermions at non-zero density, and is found in all metals. Its basic characteristics can already be understood in a simple free fermion picture. Non-interacting fermions occupy the lowest energy single particle states, consistent with the exclusion principle. This leads to the fundamental concept of the Fermi surface: a surface in momentum space separating the occupied and empty single fermion states. The lowest energy excitations then consist of quasiparticle excitations which are particle-like outside the Fermi surface, and hole-like inside the Fermi surface. Landau's Fermi liquid theory is a careful justification for the stability of this simple picture in the presence of interactions between fermions.

The purpose of this chapter is to describe two paradigms of symmetry breaking quantum transitions in Fermi liquids. In the first class, studied in Section II,

the broken symmetry is related to the point-group symmetry of the crystal, while translational symmetry is preserved; consequently the order parameter resides at zero wavevector. In the second class, studied in Section III, the order parameter is at a finite wavevector, and so translational symmetry is also broken. We will find that these transitions have distinct effects on the Fermi surface, and so lead to very different critical theories. We will study both critical theories using a simple example in each class, both motivated by the physics of the cuprate superconductors. For the first class we will consider the case of Ising nematic ordering, while in the second class we will consider the onset of spin density wave order.

Among our aims is to understand the possible breakdown of Landau's Fermi liquid theory in Fermi gases. The most prominent example of this breakdown is in spatial dimension $d = 1$, where we generically obtain (not necessarily near any quantum phase transitions) a different quantum state known as the Tomonaga-Luttinger liquid. We will meet examples of Fermi liquid breakdown in $d \geq 2$ in the present chapter.

A comprehensive theoretical treatment of symmetry breaking transitions in a Fermi liquid was given by Hertz [1], although many important points were anticipated in earlier work [2–5]. We will review this treatment here, adapted to our field-theoretic approach. A key step in Hertz's work is to completely integrate out the fermionic excitations near the Fermi surface, resulting in an effective action for the order parameter characterizing the symmetry breaking alone. Such an approach seems natural from the perspective of the classical phase transitions, in which we

need only pay attention to the low energy fluctuations of the order parameter. However, here we also have the low energy quasiparticles near the Fermi surface: they are not associated directly with the broken symmetry, but their existence is protected by the requirement of the presence of a Fermi surface. It seems dangerous to integrate them out, and it would be preferable to make them active participants in the critical theory. This is a subtle question which we will address carefully in the present chapter. The main conclusion will be that the Hertz's strategy remains largely correct in $d \geq 3$, but that it fails badly in the important case of $d = 2$. This conclusion applies to both classes of symmetry breaking transitions in a Fermi liquid: with order parameters at zero and non-zero momentum.

I. FERMI LIQUID THEORY

Let us begin with a review of some basic ideas from the Fermi liquid theory of interacting fermions in d dimensions. We consider spin-1/2 fermions c_{ka} with momentum k and spin $a =\uparrow, \downarrow$ and dispersion ε_k. Thus the non-interacting fermions are described by the action

$$\mathcal{S}_c = \int d\tau \int \frac{d^d k}{(2\pi)^d} c^\dagger_{ka} \left(\frac{\partial}{\partial \tau} + \varepsilon_k \right) c_{ka}, \tag{1}$$

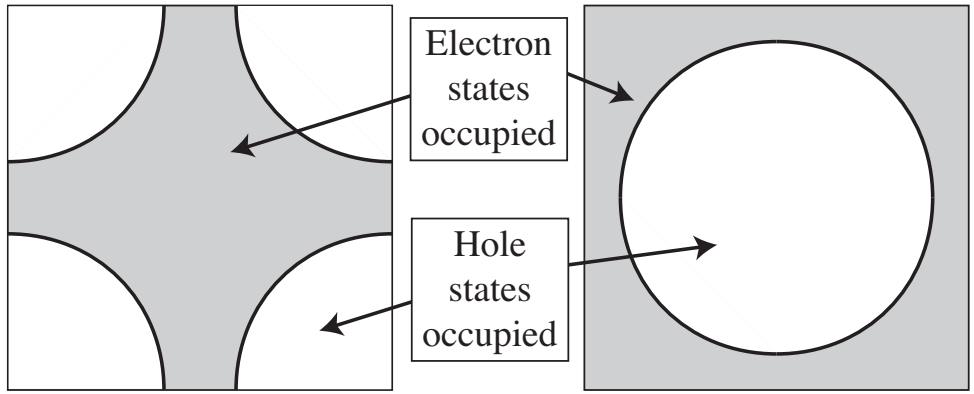

FIG. 1: Two views of the Fermi surface of the cuprate superconductors (hole and electron doped). The chemical potential is included in the dispersion ε_k, and so the Fermi surface is determined by $\varepsilon_k = 0$. The left panel has the momentum $k = (0, 0)$ (the "Γ point") in the center of the square Brillouin zone, while the right panel has the Γ point at the left edge. The momenta with both up and down electron states occupied are shaded gray.

As an example it is useful to keep in mind the dispersion ε_k appropriate for the cuprate superconductors, which is shown in Fig. 1. The fermion Green's function under the free fermion action $\mathcal{S}_c$ has the simple form

$$G_0(k, \omega_n) = \frac{1}{-i\omega_n + \varepsilon_k} \tag{2}$$

After analytically continuing to real frequencies, we observe that this Green's function has a pole at energy ε_k with residue 1. Thus there are quasiparticle excitations

with residue $\mathcal{A} = 1$, much like those found in the strong or weak coupling expansions of the quantum Ising model. However, unlike those excitations, these quasiparticles can have both positive and negative energies, as ε_k can have either sign; the Fermi surface is the locus of points where ε_k changes sign. The positive energy qausiparticles are electron-like, while those with negative energy are hole-like *i.e.* they correspond to the absence of an electron. Note that the existence of negative energy quasiparticles is not an indication of the instability of the ground state. All true excitation energies are positive: the excitations are electron-like on one side of the Fermi surface, and hole-like on the other side. It is just convenient to combine the electron and hole quasiparticles within a single Green's function, by identifying hole-like quasiparticles with negative energy electron-quasiparticles.

We now wish to examine the stability of quasiparticles to interactions between them. In keeping with the strategy followed in this book, this should be preceded by an effective action for the low energy quasiparticles. The latter is usually done by a gradient expansion, leading to an effective field theory. However, here we face a unique difficulty: there are zero energy quasiparticles along a $d-1$ dimensional Fermi surface identified by $\varepsilon_k = 0$. It would therefore seem that we should expand about all points on the Fermi surface. This is indeed the strategy followed in textbook treatments of Fermi liquid theory: we measure momenta, $k_\perp$, from the Fermi surface, choose a cutoff so that $|k_\perp| < \Lambda$, and then perform an RG which reduces the value of Λ [6]. This procedure is illustrated in Fig. 2. Formally, for each direction

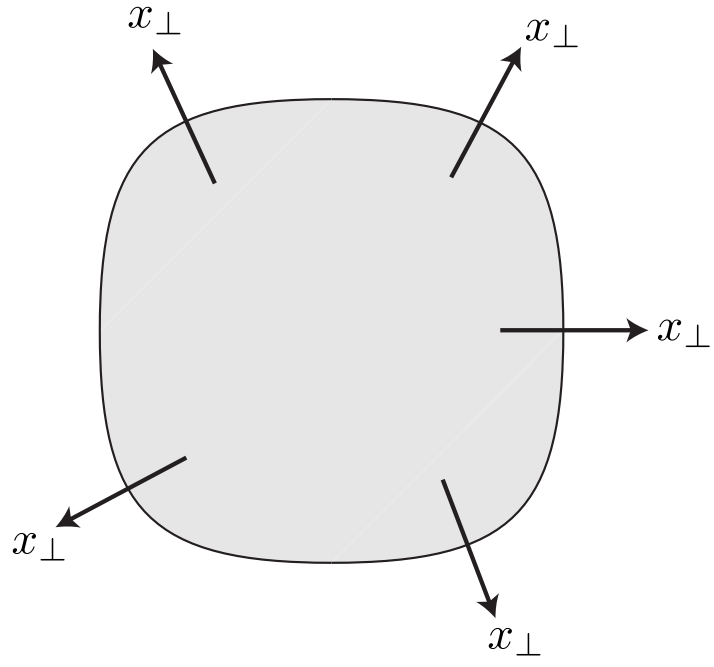

FIG. 2: Traditional low energy limit of Fermi liquid theory. The Fermi surface has one dimensional chiral fermions on every point, moving along the direction $x_\perp$. There fermions are present for momenta $|k_\perp| < \Lambda$; *i.e.* in a momentum shell of width 2Λ around the Fermi surface.

$\hat{n}$, we define the position of the Fermi surface by the wavevector $\vec{k}_F(\hat{n})$, so that $\hat{n} = \vec{k}_F(\hat{n})/|\vec{k}_F(\hat{n})|$. Then we identify wavevectors near the Fermi surface by

$$\vec{k} = \vec{k}_F(\hat{n}) + k_\perp \, \hat{n} \tag{3}$$

Now we should expand in small momenta $k_\perp$. For this, we define the infinite set of

fields $\psi_{\hat{n}a}(k_\perp)$, which are labeled by the spin a and the direction $\hat{n}$, related to the fermions c by

$$c_{\vec{k}a} = \frac{1}{\sqrt{S_F}} \psi_{\hat{n}a}(k_\perp), \tag{4}$$

where $\vec{k}$ and $k_\perp$ are related by (3), and S_F is the area of the Fermi surface. Inserting (4) into (1), expanding in $k_\perp$, and Fourier transforming to real space $x_\perp$, we obtain the low energy theory

$$\mathcal{S}_{\rm FL} = \int d\Omega_{\hat{n}} \int dx_\perp \psi^\dagger_{\hat{n}a}(x_\perp) \left(\frac{\partial}{\partial \tau} - i v_F(\hat{n}) \frac{\partial}{\partial x_\perp} \right) \psi_{\hat{n}a}(x_\perp), \tag{5}$$

where the Fermi velocity is energy gradient on the Fermi surface $v_F(\hat{n}) = |\nabla_k \varepsilon_{\vec{k}_F(\hat{n})}|$. For each $\hat{n}$, (5) describes fermions moving along the single dimension $x_\perp$ with the Fermi velocity: this is a one-dimensional chiral fermion; the 'chiral' refers to the fact that the fermion only moves in the positive $x_\perp$ direction, and not the negative $x_\perp$ direction. In other words, the low energy theory of the Fermi liquid is an infinite set of one-dimensional chiral fermions, one chiral fermion for each point on the Fermi surface.

Apart from the free Fermi term in (5), Landau's Fermi liquid theory also allows for contact interactions between chiral fermions along different directions [6]. These

are labeled by the Landau parameters, and lead only to shifts in the quasiparticle energies which depend upon the densities of the other quasiparticles. Such shifts are important when computing the response of the Fermi liquid to external density or spin perturbations. However, the resulting fixed-point action of Fermi liquid theory does not offer a route to computing the decay of quasiparticles: the stability of the quasiparticles is implicitly assumed in the fixed point theory. Our primary purpose here is to verify the stability of the quasiparticles, so that we will be prepared for the breakdown of Fermi liquid theory at quantum critical points. So we refer the reader to the many textbook treatments of the traditional formulation of Landua's Fermi liquid theory, and turn to an alternative analysis below.

A shortcoming of the effective action (5) is that it only includes the dispersion of the fermions transverse to the Fermi surface. Thus, if we discretize the directions $\hat{n}$, and pick a given point on the Fermi surface, the Fermi surface is effectively *flat* at that point. We will shortly see that the curvature of the Fermi surface is important in understanding the decay and breakdown of quasiparticles. Thus we have to take the continuum scaling limit in a manner which keeps the curvature of the Fermi surface fixed, and does not scale it to zero. For this, as shown in Fig. 3, we focus attention on a single arc of the Fermi surface in the vicinity of any chosen point $\vec{k}_0$. We will show in Section I A that the results are independent of the choice of $\vec{k}_0$ on the Fermi surface, but we defer that issue for now. Then we will choose our cutoff Λ to scale towards the single point k_0 (the cutoff will be defined more carefully

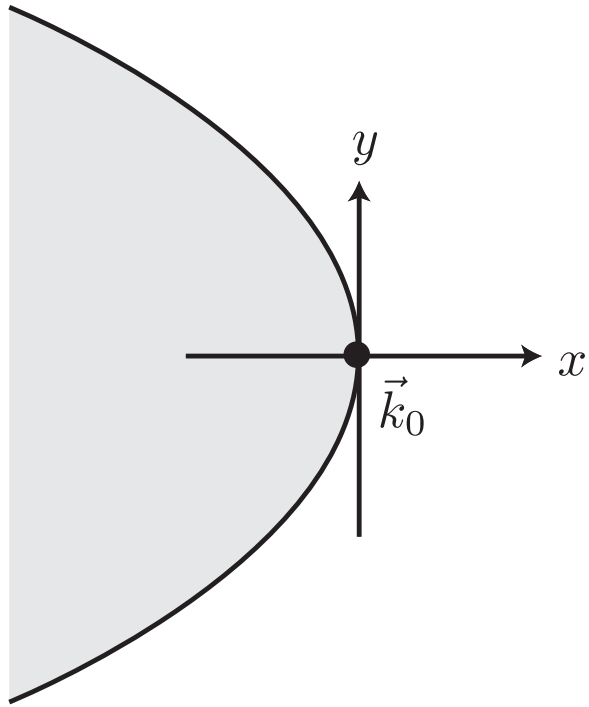

FIG. 3: Alternative low energy formulation of Fermi liquid theory. We focus on an extended patch of the Fermi surface, and expand in momenta about the point $\vec{k}_0$ on the Fermi surface. This yields a theory of d-dimensional fermions ψ in (7), with dispersion (14). The co-ordinate y represents the $d-1$ dimensions parallel to the Fermi surface.

below), rather than scaling to all points on the Fermi surface, as we did for (5).

With $\vec{k}_0$ chosen as Fig. 3, let us now define our low energy theory and scaling limit [7]. Unlike the one-dimensional chiral fermions which appeared in (5), we

will now use a d dimensional fermion $\psi_a(x, y)$. Here x is the one dimensional co-ordinate orthogonal to the Fermi surface, and $\vec{y}$ represents the $(d-1)$-dimensional transverse co-ordinates. After Fourier transformations, this fermion is related to the underlying fermions c_{ka} simply by

$$\psi_a(k) = c_{\vec{k}_0+\vec{k},a} \tag{6}$$

In other words, we only shift the origin of momentum space from $\vec{k} = 0$ to $\vec{k} = \vec{k}_0$. Inserting (6) in (1), and expanding the dispersion in the vicinity of $\vec{k}_0$ (contrast to the expansion away from all points on the Fermi surface in (5)), we obtain the low energy theory

$$\mathcal{S}_0 = \int d\tau \int dx \int d^{d-1}y \; \psi_a^\dagger \left(\zeta \frac{\partial}{\partial \tau} - iv_F \frac{\partial}{\partial x} - \frac{\kappa}{2} \nabla_y^2 \right) \psi_a. \tag{7}$$

We have added a co-efficient ζ to the temporal gradient term for future convenience: we are interested in $\zeta = 1$, but will see later that in non-Fermi liquid states it is convenient to allow ζ to renormalize. Notice the additional second-order gradients in y which were missing from (5): the co-efficient κ is proportional to the curvature of the Fermi surface at $\vec{k}_0$. Also, as we have already noted, the fermion field in (7) is d-dimensional, while that in (5) in one-dimensional. One benefit of (7) is now

immediately evident: it has zero energy excitations when

$$v_F k_x + \kappa \frac{k_y^2}{2} = 0, \tag{8}$$

and so (8) defines the position of the Fermi surface, which is then part of the low energy theory including its curvature. Note that (7) now includes an extended portion of the Fermi surface; contrast that with (5), where the one-dimensional chiral fermion theory for each $\hat{n}$ describes only a single point on the Fermi surface.

The gradient terms in (7) define a natural momentum space cutoff, and associated scaling limit. We will take such a limit at *fixed* ζ, v_F and κ. Notice that momenta in the x direction scale as the square of the momenta in the y direction, and so we can choose $v_F^2 k_x^2 + \kappa^2 k_y^4 < \Lambda^4$. Notice that as we reduce Λ, we scale towards the single point $\vec{k}_0$ on the Fermi surface, as we required above.

It now a simple matter to apply the RG analysis to the fermion theory in (7). At fixed ζ, v_F and κ, the action (7) is invariant under the following rescalings of spacetime:

$$x' = x e^{-2\ell} \quad , \quad y' = y e^{-\ell} \quad , \quad \tau' = \tau e^{-2\ell} \tag{9}$$

Note that we have chosen the directions parallel to the Fermi surface as the ones defining the primary length scale, with $\dim[y] = -1$, and the transverse direction

has $\dim[x] = -2$. The temporal direction rescaling implies that we have the dynamic exponent $z = 2$ when measured relative to the y spatial directions. The RG invariance of (7) also requires the field rescaling

$$\psi' = \psi e^{(d+1)\ell/2}. \tag{10}$$

We now have the tools needed to determine the role of fermion interactions. The simplest contact interaction has the form

$$\mathcal{S}_1 = u_0 \int d\tau \int dx \int d^{d-1}y \; \Psi_a^\dagger \Psi_b^\dagger \Psi_b \Psi_a. \tag{11}$$

Apply the RG rescalings in (10) we find

$$u_0' = u_0 e^{(1-d)\ell}. \tag{12}$$

In other words, the interaction between the fermions u_0 is irrelevant in all dimension $d > 1$. This strongly suggests that the Fermi liquid picture of non-interacting fermions is indeed RG stable.

Let us understand the stability of Fermi liquid theory a bit better by computing corrections to the fermion Green's function in (2). Let us write the interaction corrected Green's function as

$$G(k,\omega) = \frac{1}{-\zeta\omega + \varepsilon_k - \Sigma(k,\omega)}, \tag{13}$$

where now

$$\varepsilon_k = v_F k_x + \kappa \frac{k_y^2}{2}. \tag{14}$$

To first order in u_0, the fermion self energy is real (for real frequencies), and so only modifies the quasiparticle dispersion and residue, $\mathcal{A}$, but does not destabilize the existence of the quasiparticle pole.

So let us move to second order in u_0. First, we use an RG argument. We are interested in the imaginary part of the self energy, and let us assume for now at small ω

$$\mathrm{Im}\Sigma(k=0,\omega) \sim u_0^2 \omega^p. \tag{15}$$

We determine p by scaling arguments. From (13) we know that $\dim[\Sigma] = z = 2$, and so conclude from matching dimensions in (15) that $p = d$. However, there is a subtlety here: scaling arguments only yield the powerlaws of singular corrections, and do not say anything about analytic backgrounds that may be allowed from the structure of the theory. Here, a term with $p = 2$ is permitted because $\mathrm{Im}\Sigma$ is an even function of ω. So the proper conclusion is

$$p = \min(d, 2). \tag{16}$$

The above scaling argument is fine as it stands, but cannot substitute for the insight gained by an explicit computation. The Feynman diagram contributing to

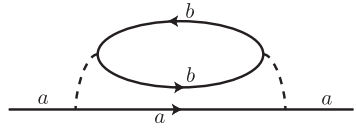

FIG. 4: Feynman diagram for the decay of quasiparticles at order u_0^2. The dashed line is the interaction u_0, and a, b are spin labels.

the quasiparticle decay at order u_0^2 is indicated in Fig. 4. We evaluate it in two stages. First we evaluate the fermion loop of the fermions with spin label b; this gives us the fermion polarizability

$$\Pi(q,\omega_n) = \int \frac{d^d k}{(2\pi)^d} \int \frac{d\epsilon_n}{2\pi} G_0(k+q, \epsilon_n + \omega_n) G_0(k, \epsilon_n). \tag{17}$$

This enters the self-energy by

$$\Sigma(k,\epsilon_n) = u_0^2 \int \frac{d^d q}{(2\pi)^d} \int \frac{d\omega_n}{2\pi} \Pi(q,\omega_n) G_0(k+q, \epsilon_n + \omega_n). \tag{18}$$

We first explicitly evaluate $\Pi(q,\omega_n)$. We will only be interested in terms that are singular in q and ω_n, and will drop regular contributions from regions of high

momentum and frequency. In this case, it is permissible to reverse the conventional order of integrating over frequency first in (17), and to first integrate over k_x. It is a simple matter to perform the integration over k_x in using the method of residues to yield

$$\begin{aligned}\Pi(q,\omega_n) &= \frac{1}{2v_F}\int \frac{d^{d-1}k_y}{(2\pi)^{d-1}}\int \frac{d\epsilon_n}{2\pi}\frac{\mathrm{sgn}(\epsilon_n+\omega_n)-\mathrm{sgn}(\epsilon_n)}{\left(\zeta\omega_n + iv_Fq_x + i\kappa q_y^2/2 + i\kappa\vec{q}_y\cdot\vec{k}_y\right)} \\ &= \frac{|\omega_n|}{2\pi v_F}\int \frac{d^{d-1}k_y}{(2\pi)^{d-1}}\frac{1}{\left(\zeta\omega_n + iv_Fq_x + i\kappa q_y^2/2 + i\kappa\vec{q}_y\cdot\vec{k}_y\right)}. \end{aligned} \tag{19}$$

We now integrate along the component of $\vec{k}_y$ parallel to the direction of $\vec{q}_y$ to obtain

$$\begin{aligned}\Pi(q,\omega_n) &= \frac{|\omega_n|}{2\pi v_F\kappa|q_y|}\int \frac{d^{d-2}k_y}{(2\pi)^{d-2}} \\ &= \frac{|\omega_n|}{2\pi v_F\kappa|q_y|}\Lambda^{d-2} \end{aligned} \tag{20}$$

Note that in $d=2$ the last non-universal factor is not present, and the result for Π is universal with $\Lambda^{d-2}=1$. Note also that ζ has dropped out of the result Π: this will be important in our subsequent treatment of quantum critical points.

Now we insert (20) into (18). After evaluating the integral over q_x we obtain

$$\begin{aligned}\Sigma(k,\omega_n) &= i\,\frac{u_0^2}{2\pi v_F^2\kappa}\int\frac{d^{d-1}q_y}{(2\pi)^{d-1}}\int\frac{d\epsilon_n}{2\pi}\frac{\mathrm{sgn}(\epsilon_n+\omega_n)|\epsilon_n|}{|q_y|}\\ &= i\,\mathrm{sgn}(\omega_n)\omega_n^2\,\frac{u_0^2}{4\pi v_F^2\kappa}\int\frac{d^{d-1}q_y}{(2\pi)^{d-1}}\frac{1}{|q_y|}\\ &= i\,\mathrm{sgn}(\omega_n)\omega_n^2\,\frac{u_0^2}{4\pi v_F^2\kappa}\Lambda^{d-2}\quad,\quad d>2. \end{aligned}\tag{21}$$

Again, ζ has dropped out. This result is in perfect accord with the scaling arguments in (15) and (16).

Let us consider the important case $d=2$. There is an infrared divergence in the q_y integral in (21) at small q_y. This is only cutoff after we include a self-consistent damping of the quasiparticle propagators in the Feynman diagram of Fig. 4, rather than the bare propagators we have used above. After including this damping, we expect that (15) will be modified to

$$\mathrm{Im}\Sigma(k,\omega)\sim u_0^2\omega^2\log\left(\frac{\Lambda}{u_0|\omega|}\right)\quad,\quad d=2;\tag{22}$$

thus the scaling result is modified by a logarithm in $d=2$.

With $\mathrm{Im}\Sigma \sim u_0^2\omega^2$ (up to logarithms) , we can now easily examine the fate of the quasiparticles from (13). From (13), we see that the quasiparticle pole is always broadened: the width of the quasiparticle peak is $\sim u_0^2\varepsilon_k^2$ for a quasiparticle with energy $\omega = \varepsilon_k$. Thus the quasiparticle width vanishes as the square of the distance from the Fermi surface. Asymptotically close to the Fermi surface, the quasiparticle width is much smaller than the quasiparticle energy: this is sufficient to regard the quasiparticle as a sharp excitation, and confirm the validity of Landau's Fermi liquid theory.

An important and frequently used diagnostic of the stability of the quasiparticle is the discontinuity in the fermion momentum distribution function $n(k) = \langle c_{ka}^\dagger c_{ka}\rangle$. This can be computed from the real frequency Green's function $G(k,\omega)$ by (here we set $\zeta = 1$)

$$n(k) = \int_{-\infty}^{0} \frac{d\omega}{(2\pi)} \mathrm{Im}G(k,\omega). \tag{23}$$

Assuming a pole in the Green's function of the form

$$G(k,\omega) = \frac{\mathcal{A}}{-\omega + \varepsilon_k + ic\omega^2} + \ldots \tag{24}$$

we find a step discontinuity in the momentum distribution function at the Fermi

surface

$$n(k) = \mathcal{A}\theta(-\varepsilon_k) + \dots \tag{25}$$

of strength $\mathcal{A}$.

A. Independence on choice of $\vec{k}_0$

Our theory of the Fermi liquid state is now contained in the action $\mathcal{S}_0 + \mathcal{S}_1$ defined by (7) and (11). It focused on an arc of the Fermi surface, as shown in Fig. 3, and then expanded in gradients about the point $\vec{k}_0$ on the Fermi surface. To complete our discussion, we now wish to show that the theory is *independent* of the choice of $\vec{k}_0$.

As shown in Fig. 5, we could equally well have defined the theory about the point $\vec{k}_0'$ on the Fermi surface. Consistency requires that the fermion Green's function at the point P should have the same value whether it is computed using the theory at $\vec{k}_0$ or at $\vec{k}_0'$. This section will show that this is indeed the case.

Note that such a consistency requirement is not present for the representation in terms of chiral one-dimensional fermions in Fig. 2. There, each point in the momentum space is associated only with a single one-dimensional theory. It is our use of a d-dimensional theory which induces our redundant description.

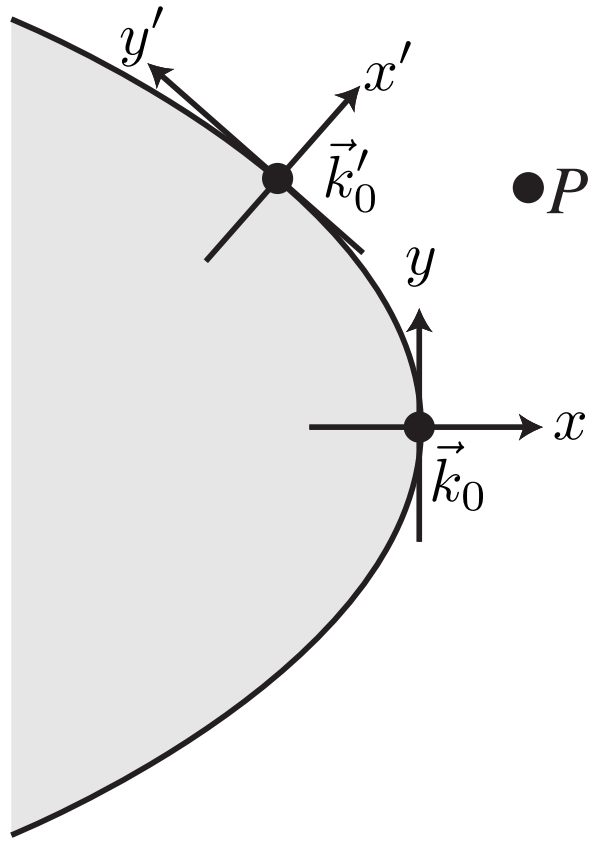

FIG. 5: The fermion correlator at the point P can be described either in terms of the field theory $\mathcal{S}_0 + \mathcal{S}_1$ at $\vec{k}_0$, or that at $\vec{k}_1$.

Let us choose our momentum space co-ordinates centered at $\vec{k}_0$, and let $\vec{k}'_0 = (k_x, k_y)$ in this co-ordinate system. Because $\vec{k}'_0$ is on the Fermi surface, (8) is obeyed. Now let the point P in Fig. 5 have co-ordinates (p_x, p_y) relative to $\vec{k}_0$, and

co-ordinates (p'_x, p'_y) relative to $\vec{k}'_0$. The latter are obtained from the old co-ordinates by a shift in origin followed by a rotation by an angle θ, where $\tan\theta = \kappa k_y/v_F$; this yields

$$\begin{aligned} p'_x &= p_x - k_x + (\kappa/v_F)\vec{k}_y \cdot (\vec{p}_y - \vec{k}_y) \\ \vec{p}'_y &= \vec{p}_y - \vec{k}_y \quad , \end{aligned} \tag{26}$$

where we only keep terms to the needed accuracy of $\mathcal{O}(x, y^2)$. The equality of the physics in the two co-ordinate systems implies that the Green's function of the theory $\mathcal{S}_0 + \mathcal{S}_1$ must satisfy

$$G((p_x, p_y), \omega) = G((p'_x, p'_y), \omega) \tag{27}$$

for any momenta p, p' related by (26) and any k obeying (8). A simpler statement of the constraint follows from the easily verified identity

$$v_F p_x + \frac{\kappa}{2} p_y^2 = v_F p'_x + \frac{\kappa}{2} p_y'^2 \tag{28}$$

Thus, the Green's function should not depend separately on the momenta, but on the quasiparticle energy in (14) alone:

$$G((p_x, p_y), \omega) = G(\varepsilon_p, \omega). \tag{29}$$

We will now prove (29) is true. The result relies upon the invariance of $\mathcal{S}_0 + \mathcal{S}_1$ on the following transformation

$$\psi(x, \vec{y}) \to \exp\left(-i\frac{v_F}{\kappa}\left(\vec{\theta}\cdot\vec{y} + \frac{\theta^2}{2}x\right)\right)\psi(x, \vec{y} + \vec{\theta}\,x), \tag{30}$$

where θ is an arbitrary $d-1$ dimensional vector; this invariance is easily verified by direct substitution in (7) and (11). The change in the arguments of ψ shows that this transformations corresponds to a local rotation of the Fermi surface, which effectively moves the point $\vec{k}_0$ to a neighboring point. Now taking the Fourier transform of (30), we immediately establish (27) and (29).

II. ISING-NEMATIC ORDERING

Having established the stability of quasiparticles in the Fermi liquid, we turn to the first of the symmetry breaking transitions of this chapter. We consider one of the simplest order parameters at zero wavevector: the breaking of lattice rotation symmetry. In two dimensions, a simple choice is the change from "square" to "rectangular" symmetry. In higher dimensions, we consider the same symmetry breaking in the x, y plane embedded in the higher-dimensional space.

We consider an Ising-nematic transition driven by strong interactions among the electrons. The symmetry breaking is characterized by the real scalar field ϕ, which

is described as before by the action $\mathcal{S}_\phi$

$$\mathcal{S}_\phi = \int d^d x d\tau \left[\frac{1}{2} \left((\partial_\tau \phi)^2 + c^2 (\partial_x \phi)^2 + c^2 (\partial_y \phi)^2 + r \phi^2 \right) + \frac{u}{24} \phi^4 \right], \tag{31}$$

There is a Fermi surface of fermions c_{ka}, described here by $\mathcal{S}_c$ in (1). Finally, we need to couple the Ising order ϕ to the fermions. This can be deduced by symmetry considerations. A convenient choice is

$$\mathcal{S}_{c\phi} = \int d\tau \int \frac{d^d k d^d q}{(2\pi)^{2d}} d(k) \phi(q) c^\dagger_{k+q/2,a} c_{k-q/2,a}. \tag{32}$$

The momentum dependent form factor, $d(k)$, can be any even parity function which changes sign under $x \leftrightarrow y$, as is required by the symmetry properties of ϕ; a simple choice is $d(k) \sim \cos k_x - \cos k_y$. The integral over q is over small momenta, while that over k extends over the entire Brillouin zone.

The theory for the nematic ordering transition is now described by $\mathcal{S}_c + \mathcal{S}_\phi + \mathcal{S}_{c\phi}$ in Eqs. (1), (31), and (32), and will form the basis of the discussion in the remainder of this chapter. A schematic phase diagram as a function of the coupling s in $\mathcal{S}_\phi$ and temperature T is shown in Fig. 6. Note that there is a line of Ising phase transitions at $T = T_c$: this transition is in the same universality class as the classical two-dimensional Ising model. However, quantum effects and fermionic excitations are crucial at $T = 0$ critical point at $r = r_c$ and its associated quantum critical region.

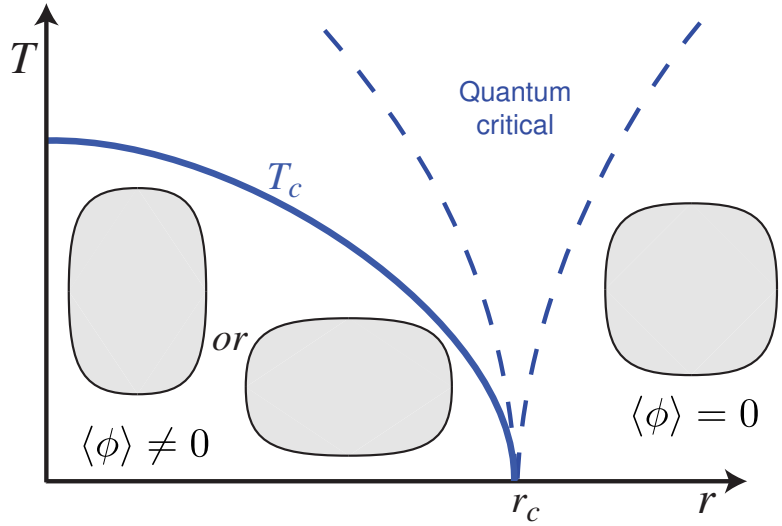

FIG. 6: Phase diagram of Ising nematic ordering in a metal as a function of the coupling s in $\mathcal{S}_\phi$ and temperature T. The Fermi surface for $r > 0$ is as in the overdoped region of the cuprates, with the shaded region indicating the occupied hole (or empty electron) states (compare Fig. 1). The choice between the two quadrapolar distortions of the Fermi surface is determined by the sign of $\langle\phi\rangle$. The line of $T > 0$ phase transitions at T_c is described by Onsager's solution of the classical two-dimensional Ising model. We are interested here in the quantum critical point at $r = r_c$, which controls the quantum-critical region.

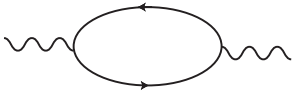

FIG. 7: Fermion loop contribution to the action of the order parameter ϕ. The wavy line is ϕ.

A. Hertz theory

As indicated in the introduction, Hertz's strategy is to integrate out all the fermionic excitations, and derive an effective action for the Ising order parameter ϕ.

The integration is easily performed using our Fermi liquid theory results in Section I. The important term is the fermion loop contribution to the ϕ^2 term in the effective action, and this is given by the Feynman diagram in Fig. 7. We can determine the structure of fermion loop integral by taking the continuum limit of fermion theory in a Fermi surface patch about $\vec{k}_0$ as in (7), and then adding up the contributions of all the patches. For a given patch, the fermion loop contributes $d^2(k_0)\Pi(q,\omega)$, where Π is the fermion polarizability in (17). Using the result for Π in (20), averaging over different patches on the Fermi surface, and combining with the terms of the ϕ action in (31), we obtain the Hertz action for the order parameter

at the Ising-nematic quantum critical point in d dimensions:

$$\mathcal{S}_H = \int \frac{d^d k}{(2\pi)^d} T \sum_{\omega_n} \frac{1}{2} \left[k^2 + \gamma \frac{|\omega_n|}{|k|} + r \right] |\phi(k, \omega_n)|^2 + \frac{u}{24} \int d^d x d\tau \phi^4(x, \tau). \quad (33)$$

Compared to (31), the crucial new term is the one proportional to γ, which represents the non-local consequences of low energy particle-hole excitations near the Fermi surface; the value of γ is determined from an average of the coefficient in (20) over the Fermi surface. In a system with a spherical Fermi surface, the $|k|$ in the denominator is simple $\sqrt{\vec{k}^2}$, arising from the average of (20) over different patches. However, without spherical symmetry, it is a more complex function which depends upon the details of the Fermi surface structure. Nevertheless, it retains the property of being an even function of k with scaling dimension 1, and that is all that we shall need below.

We are now ready to perform an RG analysis of $\mathcal{S}_H$. We begin with an analysis of the Gaussian part of $\mathcal{S}_H$, which is scale-invariant at $r = 0$, under the transformations:

$$x' = x e^{-\ell} \quad , \quad \tau' = \tau e^{-z\ell} \quad , \quad \phi' = \phi e^{(d+z-2)\ell/2} \quad (34)$$

with dynamic critical exponent $z = 3$. This exponent can also be understood from the characteristic frequency scale $\omega \sim k^3$ emerging from a comparison of the first two terms in $\mathcal{S}_H$. With the transformations in (34), we see that the quartic coupling has scaling dimension

$$\dim[u] = 4 - d - z. \tag{35}$$

In other words, with $z = 3$, the Gaussian fixed point is stable for all $d > 1$. All computations in this chapter have implicitly assumed that $d > 1$, and the present approach is not sensible in $d = 1$. So the Gaussian theory appears to describe the quantum critical point for all values of d. This is one of Hertz's primary conclusions.

We will argue below that the above conclusion is not correct. The Gaussian fixed point does, in fact, yield a proper description in $d = 3$. However, in the physically important case of $d = 2$, the Hertz approach fails.

B. Fate of the fermions

Our analysis of the stability of the Gaussian fixed point of the Hertz theory relied on the irrelevance of the quartic coupling u between the bosons. However, there are also fermionic quasiparticle excitations in the underlying theory, and it is important to apply the RG to these excitations too. In particular, they couple to ϕ via the

"Yukawa" coupling of $\mathcal{S}_{c\phi}$ in (32), and to establish the stability of the Gaussian fixed point we need to examine the scaling dimension of $d(k)$ on the Fermi surface.

Answering this question requires a continuum theory for the fermionic sector also, and its coupling to the bosonic sector. Fortunately, we can now directly use the continuum limit presented in Section I. We pick a Fermi surface patch centered at the momentum $\vec{k}_0$, and describe the low energy fermionic quasiparticles by $\mathcal{S}_0$ in (7). Next, we apply the substitution (6) to (32), and obtain the Yukawa coupling

$$\mathcal{S}_{\psi\phi} = \lambda \int d\tau \int dx \int d^{d-1}y \, \phi \, \psi_a^\dagger \psi_a \tag{36}$$

where $\lambda = d(k_0)$. Finally, we also need to distinguish the directions parallel and transverse to the Fermi surface in $\mathcal{S}_H$, and so write its Gaussian part as

$$\mathcal{S}_{HG} = \frac{1}{2} \int \frac{dk_x}{(2\pi)} \int \frac{d^{d-1}k_y}{(2\pi)^{d-1}} \int \frac{d\omega_n}{2\pi} \left[k_y^2 + \gamma \frac{|\omega_n|}{|k_y|} + r \right] |\phi(k, \omega_n)|^2. \tag{37}$$

We have dropped the k_x dependence in (18) because it is irrelevant compared to the k_y dependence under the rescaling (9).

Now our task it so determine the scaling dimension of λ under the theory $\mathcal{S}_0 + \mathcal{S}_{HG} + \mathcal{S}_{\psi\phi}$ defined in (7), (37), and (36).

We scale x and y as in (9). For the rescaling of time, we clearly need to focus on the critical excitations of the Ising nematic order, which have dynamic exponent

$z = 3$. Thus we choose

$$x' = xe^{-2\ell} \quad , \quad y' = ye^{-\ell} \quad , \quad \tau' = \tau e^{-3\ell} \tag{38}$$

An immediate consequence is that the coefficient ζ of the temporal derivative term in $\mathcal{S}_0$ in (7) is no longer invariant under the RG: it has scaling dimension

$$\dim[\zeta] = -1 \tag{39}$$

and so scales to zero. Thus this temporal derivative is irrelevant at the Ising nematic quantum critical point. It is important at this point that our derivation of $\mathcal{S}_H$ in (33) showed that all terms had a finite limit as $\zeta \to 0$: in fact, the damping coefficient γ was shown to be independent of ζ in (20). Thus setting $\zeta = 0$ seems safe now, although this conclusion will have to be re-examined at higher orders.

With these choices for the spacetime rescalings, it is a simple matter to compute the rescalings of the fields from their respect Gaussian actions:

$$\dim[\psi] = (d+2)/2 \quad , \quad \dim[\phi] = (d+2)/2. \tag{40}$$

Finally, we obtain the needed renormalization of the fermion-boson coupling in (36)

$$\dim[\lambda] = \frac{(2-d)}{2}. \tag{41}$$

So only for $d > 2$ is the Gaussian action stable to the presence of the cubic nonlinearity associated with the fermion-boson coupling. This is the primary conclusion of this subsection.

For $d > 2$, the above arguments suggest that we can estimate the fate of the fermionic quasiparticles in a perturbation theory in λ. Let us first try to guess the structure of the answer using scaling arguments; we expect

$$\mathrm{Im}\Sigma \sim \lambda^2 \omega^p. \tag{42}$$

Matching scaling dimensions with $\dim[\Sigma] = 2$ (because $\dim[k_x] = \dim[k_y^2] = 2$), $\dim[\omega] = 3$ and (41), we obtain

$$p = \frac{d}{3}. \tag{43}$$

In $d = 3$, the integer value of p suggests that there should be additional logarithms, and we will indeed see this in an explicit computation below. Examination of the quasiparticle spectral weight using (13), and as discussed below (22) shows that the quasiparticles are only marginally well defined with a width of the same order as the quasiparticle energy upon approaching the Fermi surface. Such states were named 'marginal Fermi liquids' [8], but the present argument shows this terminology is a misnomer in the RG sense: the coupling λ is irrelevant and not marginal. The RG argument also has a bonus in implying that higher orders in λ will only

produce higher powers of ω in the self-energy; perturbation theory about the Gaussian fixed point directly yields the terms most important in the infrared already at low order in the expansion.

The situation is very different in $d = 2$. In this case $\mathrm{Im}\Sigma \sim \omega^{2/3}$, and so it is now clear from (22) that quasiparticle is no longer well defined, and we are dealing with a non-Fermi liquid. Applying (23), we find that the momentum distribution function does not have a step discontinuity on the Fermi surface; there is a weaker power-law singularity with

$$n(k) \sim \mathrm{sgn}(-\varepsilon_k)|\varepsilon_k|^{1/3}. \tag{44}$$

Importantly, the scaling dimension of the boson-fermion coupling λ is 0, and so it is not clear whether perturbation theory in λ is reliable. The implication is that the critical theory should be formulated at a fixed λ, and that the perturbative Hertz approach has broken down. We will turn to a discussion of the needed critical field theory in Section II C.

However, before we turn to that crucial question, we need to verify the scaling estimate for the self energy in (42) by an explicit computation. The needed contribution to the self energy at order λ^2 is given by the Feynman diagram in Fig. 8 which evaluates to

$$\Sigma(k, \omega_n) = \lambda^2 \int \frac{d^d q}{(2\pi)^d} \int \frac{d\epsilon_n}{2\pi} \frac{1}{q_y^2 + \gamma|\epsilon_n|/|q_y|} G_0(k + q, \epsilon_n + \omega_n) \tag{45}$$

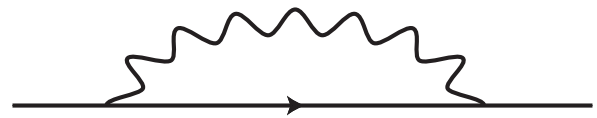

FIG. 8: Order λ^2 contribution to the fermion self energy.

This can be evaluated by the same methods used for (18). Integrating over q_x we find the analog of (21)

$$\Sigma(k,\omega_n) = i\,\frac{\lambda^2}{v_F}\int\frac{d^{d-1}q_y}{(2\pi)^{d-1}}\int\frac{d\epsilon_n}{2\pi}\,\frac{\mathrm{sgn}(\epsilon_n+\omega_n)|q_y|}{|q_y|^3+\gamma|\epsilon_n|}$$
$$= i\,\frac{\lambda^2}{\pi v_F\gamma}\mathrm{sgn}(\omega_n)\int\frac{d^{d-1}q_y}{(2\pi)^{d-1}}|q_y|\ln\left(\frac{|q_y|^3+\gamma|\omega_n|}{|q_y|^3}\right). \qquad (46)$$

Evaluation of the q_y integral yields a result which agrees with (42) and (43) in $d=2$, and with the expected logarithmic corrections in $d=3$. In the physically important case of $d=2$, the q_y integral evaluates to

$$\Sigma(k,\omega_n) = \frac{\lambda^2}{\pi v_F\gamma^{1/3}\sqrt{3}}\mathrm{sgn}(\omega_n)|\omega_n|^{2/3} \quad , \quad d=2, \qquad (47)$$

in agreement with (43).

C. Non-Fermi liquid criticality in $d = 2$

Section II B established that a perturbative analysis in the fermion-boson coupling λ, in the spirit of the familiar "random-phase-approximation" (RPA) of many body physics, led to a valid theory of the Ising-nematic quantum critical point in $d = 3$. However, the RPA-like Hertz approach broke down in $d = 2$. Here we will provide a field-theoretic description of the quantum criticality in $d = 2$, using the approach proposed in Ref. [7].

An important feature of the discussion in Section II B was that the low energy fermion modes at the Fermi surface point $\vec{k}_0$ coupled most strongly to ϕ fluctuations with momenta parallel to the Fermi surface. This is clear from the k_y dependence of $\mathcal{S}_{HG}$ in (37). Physically, this is because a fermion at $\vec{k}_0$ scattered by ϕ by momentum k tangent to the Fermi surface only changes its energy $\sim k^2$, while in all other directions its energy change $\sim k$. Consistent with this, if we compute the induced four-point ϕ vertex in the theory $\mathcal{S}_0 + \mathcal{S}_{HG} + \mathcal{S}_{\psi\phi}$, we find an enhancement dependent upon on the ϕ momenta only if the momenta are parallel or anti-parallel. This suggests that all couplings between ϕ fluctuations with non-collinear momenta, such as *e. g.* those induced by the u term in (33), are formally irrelevant, just as in the Hertz theory. This asymptotic decoupling indicates that we may treat non-collinear directions of ϕ in separate critical theories. Thus we end up with an infinite number of 2+1 dimensional field theories, labeled by the momentum

direction of ϕ.

The reader will recall our discussion of an infinite number of 1+1 dimensional field theories of chiral fermions in our discussion of Fermi liquid theory associated with Eq. (5). A crucial difference here is that we have an infinite number of 2+1 dimensional field theories: this is needed because, as discussed above, the dominant scattering processes for the fermions are tangent to the Fermi surface. The present description necessarily induces a redundant description: however, by a simple generalization of the arguments in Section I A, we will see that the redundant description is consistent.

So let us focus on a given direction $\vec{q}$ of the momentum carried by ϕ and derive the associated critical theory, as illustrated in Fig. 9. Such a ϕ field will couple most strongly to fermions near *two* points on the Fermi surface: those at $\vec{k}_0$ and at $-\vec{k}_0$. We generalize (6) by introducing two fermionic field $\psi_{\pm a}$ by

$$\psi_{+a}(\vec{k}) = c_{\vec{k}_0+\vec{k},a} \quad , \quad \psi_{-a}(\vec{k}) = c_{-\vec{k}_0+\vec{k},a}. \tag{48}$$

We will allow the spin index a to extend over the N values: the physical case is $N = 2$, but the large N expansion provides a useful computational tool.

Now we expand all terms in $\mathcal{S}_c + \mathcal{S}_\phi + \mathcal{S}_{c\phi}$ (defined in (1), (31), and (32)) in spatial and temporal gradients. Using the co-ordinate system illustrated in Fig. 9, performing appropriate rescaling of co-ordinates, and dropping terms which can

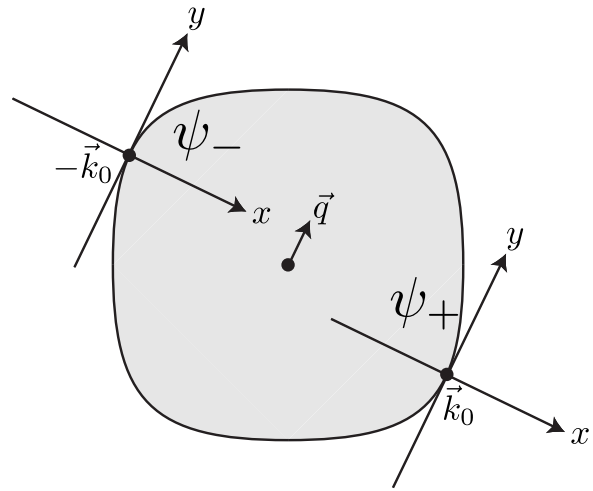

FIG. 9: A ϕ fluctuation at wavevector $\vec{q}$ couples most efficiently to the fermions $\psi_\pm$ near the Fermi surface points $\pm\vec{k}_0$.

later be easily shown to be irrelevant, we obtain the 2+1 dimensional Lagrangian

$$\begin{aligned}\mathcal{L} &= \psi^\dagger_{+a}\left(\zeta\frac{\partial}{\partial\tau} - i\frac{\partial}{\partial x} - \frac{\partial^2}{\partial y^2}\right)\psi_{+a} + \psi^\dagger_{-a}\left(\zeta\frac{\partial}{\partial\tau} + i\frac{\partial}{\partial x} - \frac{\partial^2}{\partial y^2}\right)\psi_{-a} \\ &- \lambda\,\phi\left(\psi^\dagger_{+a}\psi_{+a} + \psi^\dagger_{-a}\psi_{-a}\right) + \frac{N}{2}(\partial_y\phi)^2 + \frac{Nr}{2}\phi^2. \end{aligned} \tag{49}$$

Here ζ, λ and r are coupling constants, with r the tuning parameter across the transition; we will see that all couplings apart from r can be scaled away or set equal to unity.

A first crucial property of $\mathcal{L}$ is that it continues to have fermion Green's functions with singularities on the original Fermi surface, as established in Section I A. This follows from generalizing the symmetry (30) to

$$\phi(x,y) \to \phi(x,y+\theta x), \quad \psi_s(x,y) \to e^{-is(\frac{\theta}{2}y+\frac{\theta^2}{4}x)}\psi_s(x,y+\theta x), \tag{50}$$

where θ is now one-dimensional and $s = \pm$. This is an emergent symmetry of $\mathcal{L}$ for arbitrary shapes of the Fermi surface. An immediate consequence of (50) is that (29) is obeyed by both $\psi_\pm$, so that all singularities slide without change along the Fermi surface. Furthermore the ϕ Green's function, D, obeys

$$\langle|\phi(q,\omega)|^2\rangle \equiv D(q_x,q_y,\omega) = D(q_y,\omega) \tag{51}$$

indicating that no singular q_x dependence of ϕ is generated by the theory $\mathcal{L}$. As in Section I A, the symmetries in Eq. (50) also help establish the consistency of our description in terms of an inifinite number of 2+1 dimensional field theories.

1. Scaling theory

We will now generalize the scaling analysis of Section II B to the continuum field theory $\mathcal{L}$. Because $\mathcal{L}$ is strongly coupled, we have to allow for anomalous dimensions at all stages.

As before we choose

$$\dim[y] = -1 \quad , \quad \dim[x] = -2 \tag{52}$$

The invariance in (29) implies that no anomalous dimension appears in the relative scaling of x and y. However, we do have to allow for an anomalous dimension in time, and so keep the rescaling of the temporal co-ordinate general:

$$\dim[\tau] = -z. \tag{53}$$

Note that the dynamic critical exponent z is defined relative to the spatial co-ordinate y tangent to the Fermi surface (other investigators sometimes define it relative to the co-ordinate x normal to the Fermi surface, leading to a difference in a factor of 2). We define the engineering dimensions of the fields so that co-efficients of the y derivatives remain constant. Allowing for anomalous dimensions η_ϕ and η_ψ from loop effects we have

$$\dim[\phi] = (1 + z + \eta_\phi)/2 \quad , \quad \dim[\psi] = (1 + z + \eta_\psi)/2. \tag{54}$$

Using these transformations, we can examine the scaling dimensions of the couplings in $\mathcal{L}$ at tree level

$$\dim[\zeta] = 2 - z - \eta_\psi \quad , \quad \dim[\lambda] = (3 - z - \eta_\phi - 2\eta_\psi)/2. \tag{55}$$

We have seem from our low order loop computations in Sections II A and II B that $z = 3$. Assuming the anomalous dimensions η_ϕ and η_ψ are small, we see that the coupling ζ is strongly irrelevant. Thus we can send $\zeta \to 0$ in all our computations. However, we do not set $\zeta = 0$ at the outset, because the temporal derivative term is needed to define the proper analytic structure of the frequency loop integrals [9].

Also note that these estimates of the scaling dimensions imply $\dim[\lambda] \approx 0$. Thus the fermion and order parameter fluctuations remain strongly coupled at all scales in $d = 2$, as we anticipated in Section II B. Conversely, we can also say that the requirement of working in a theory with fixed λ implies that $z \approx 3$; this circumvents the appeal to loop computations for taking the $\zeta \to 0$ limit. With a near zero scaling dimension for λ, we cannot expand perturbatively in powers of λ.

Moving beyond tree level considerations, we note that another Ward identity obeyed by the theory $\mathcal{L}$ allows us to fix the scaling dimension of ϕ exactly. This Ward identity is linked to the fact that ϕ appears in the Yukawa coupling like the x component of a gauge field coupled to the fermions [7]. The usual arguments associated with gauge invariance then imply that $\dim[\phi] = 2$ (the same as the scaling dimension of ∂_x), and that we can work in theory in which the "gauge coupling" λ set equal to unity at all scales. Note that with this scaling dimension, we have the exact relation

$$\eta_\phi = 3 - z. \tag{56}$$

Note also that Eq. (54) now implies that $\dim[\lambda] = \eta_\psi$ at tree level, which is the

same as the tree level transformation of the spatial derivative terms. The latter terms have been set equal to unity by rescaling the fermion field, and so it is also consistent to set $\lambda = 1$ from now on.

We reach the remarkable conclusion that at the critical point $r = r_c$, $\mathcal{L}$ is independent of all coupling constants. The only parameter left is N, and we have no choice but to expand correlators in powers of $1/N$. The characterization of the critical behavior only requires computations of the exponents z and η_ψ, and associated scaling functions.

We can combine all the above results into scaling forms for the ϕ and Ψ Green's functions at the quantum critical point at $T = 0$. These are, respectively

$$D^{-1}(q_x, q_y, \omega) = q_y^{z-1} \mathcal{F}_D \left(\frac{\omega}{q_y^z} \right) \tag{57}$$

$$G_+^{-1}(q_x, q_y, \omega) = (q_x + q_y^2)^{1-\eta_\psi/2} \mathcal{F}_G \left(\frac{\omega}{(q_x + q_y^2)^{z/2}} \right), \tag{58}$$

where $\mathcal{F}_D$ and $\mathcal{F}_G$ are non-trivial scaling functions. Note that the second scaling form shows that the singularity of the fermion Green's function in momentum space is invariant along the Fermi surface, and depends only upon the distance from the Fermi surface.

We have come as far as possible by symmetry and scaling analyses alone on $\mathcal{L}$. Further results require specific computations of loop corrections, and these can only

be carried out within the context of the $1/N$ expansion. At leading order, the $1/N$ expansion reproduces the results in Section II B. It is important to note that in the notation of the present section, the results of Section II B for D and the fermion self energy turn out to be *independent* of ζ. Although ζ appears at intermediate stages, it cancels out in the final result: the reader is urged to verify this crucial feature of the theory. Consequently there is no problem in taking the $\zeta \to 0$ limit. Higher order computations are involved, and raise numerous complicated issues we do not wish to enter into here: we refer the reader to Refs. [7, 9]. It was found that $z = 3$ was preserved upto three loops, but a non-zero value for η_ψ did appear at three loop order.

III. SPIN DENSITY WAVE ORDER

We now turn to the second major class of symmetry breaking transitions of Fermi liquids: those involving an order parameter which is spatial modulated and so breaks translational symmetry. As a canonical example of such a transition we will consider spin density wave (SDW) ordering in the Hubbard Hamiltonian describing a single band on the square lattice, which was motivated by the physics of the cuprate superconductors. However, our methods and results are easily extended to other types of ordering with spatial modulations.

We have already met the analog of spin density wave ordering in insulating antif-

eromagnets. In that context it was referred to as Néel ordering, and characterized by the order parameter $\mathbf{n}$ of the O(3) quantum rotor model. In the continuum soft-spin limit, such ordering was described by the 3-component real field ϕ_α whose fluctuations were controlled by a Landau-Ginzburg action $\mathcal{S}_\phi$. The field ϕ_α will remain the order parameter for SDW ordering in a metal being considered here, and its action $\mathcal{S}_\phi$ will be an important ingredient in our theory.

Apart from the order parameter, we also have to consider the fermionic excitations near the Fermi surface, and these will be described as before by $\mathcal{S}_c$ in (1).

Finally we need to couple the c_{ka} fermions to the SDW order ϕ_α. The two sublattice Néel order on the square lattice carries momentum $\vec{K} = (\pi, \pi)$, and we can consider a general $\vec{K}$ which leads to two-sublattice SDW ordering. Other values of $\vec{K}$ lead to complex order parameter fields (rather than the real case we considered), but we will not consider this relatively straightforward generalization. Translational invariance implies that ϕ_α will scatter the fermions with momentum $\vec{K}$, and so the natural generalization of the fermion-boson coupling in (32) is

$$\mathcal{S}_{c\phi} = \int d\tau \int \frac{d^d k d^d q}{(2\pi)^{2d}} \phi_\alpha(q) \sigma^\alpha_{ab} c^\dagger_{k+K+q,a} c_{kb} + \text{c.c.} \tag{59}$$

where q is a small momentum associated with a long-wavelength SDW fluctuation, while the integral over the momentum $\vec{k}$ extends over the entire Brillouin zone.

Our complete theory for the SDW transition is $\mathcal{S}_c + \mathcal{S}_\phi + \mathcal{S}_{c\phi}$. This will form the basis of the discussion in the remainder of this section.

A. Mean field theory

The theory has two phases: the ordinary Fermi liquid with $\langle \phi_\alpha \rangle = 0$ and Fermi surface as in Fig. 1, and the SDW state with $\langle \phi_\alpha \rangle \neq 0$. We describe here the configuration of the Fermi surface in the SDW state. We replace ϕ_α by its expectation value $\langle \phi_\alpha \rangle = (0, 0, \phi)$; by rotational symmetry we can take the SDW order in the z direction without loss of generality. Now $\mathcal{S}_c + \mathcal{S}_{c\phi}$ is a bilinear in the fermions and can be diagonalized to yield a fermion band structure. The fermion Hamiltonian takes the form of a 2×2 matrix coupling together c_{ka} and $c_{k+K,a}$. Diagonalizing this matrix leads to the single fermion energy eigenvalues

$$E_k = \frac{\varepsilon_k + \varepsilon_{k+K}}{2} \pm \left(\left(\frac{\varepsilon_k + \varepsilon_{k+K}}{2} \right)^2 + \phi^2 \right)^{1/2} \tag{60}$$

We now have to occupy the lowest energy bands in this band structure, and deduce the configuration of the Fermi surface. Such a solution is illustrated in Fig 10 for the case of $\vec{K} = (\pi, \pi)$ ordering in the cuprate superconductors [10]. A key feature is

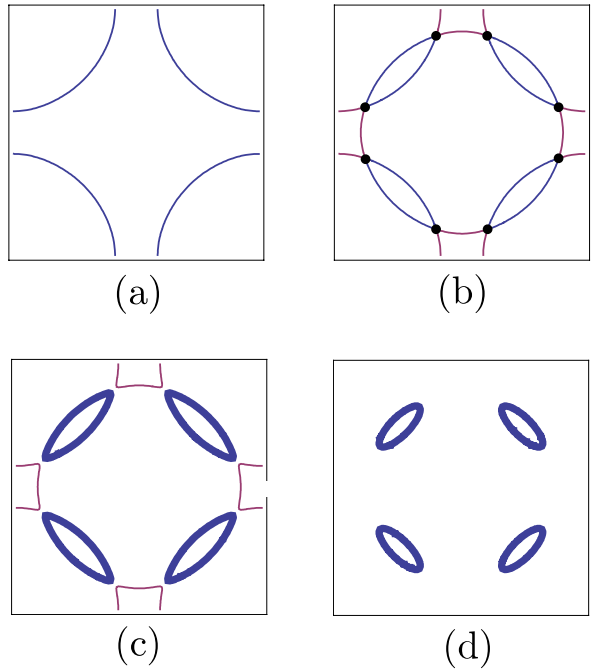

FIG. 10: The transformation of the Fermi surface of the cuprates by SDW order [10]. (a) Fermi surface without SDW order, as in Fig. 1 (b) The original Fermi surface along with the Fermi surface shifted by wavevector (π, π). These intersect at the hot spots shown by the filled circles. (c) With the onset of a non-zero spin density wave order with $\langle \phi_\alpha \rangle \neq 0$, gaps open at the hot spots leading to electron (thin lines) and hole (thick lines) pockets. (d) With increasing $|\langle \phi_\alpha \rangle|$ the electron pockets shrink to zero for the hole-doped case, leaving only hole pockets. In the electron-doped case, the hole pockets shrink to zero, leaving only electron pockets (this is not shown). Finally, in the half-filled case, the electron and hole pockets shrink to zero simultaneously.

that the original "large" Fermi surface, splits into "small" electron and hole pockets upon the onset of SDW order: this is also a generic property of SDW ordering on other lattices.

B. Continuum theory

We now wish to develop a continuum theory for the quantum critical point for the onset of SDW order, which is accompanied by a change from a large Fermi surface to small pockets, as indicated in Fig. 10. The general strategy will be similar to that in Section II, although there will be key differences which we will highlight below.

An important and new concept here is that of a "hot" manifold on the Fermi surface. As in Section II, we expect the boson-fermion coupling to be most efficient if it scatters fermions between nearly degenerate low energy states. Let us pick a point $\vec{k}_1$ on the Fermi surface, where the fermion has zero energy: this is described by d-dimensional vector upon which we impose one constraint to place it on the Fermi surface. Now the ϕ_α field will scatter this fermion to the point $\vec{k}_2 = \vec{k}_1 + K$. We require that $\vec{k}_2$ is also on the Fermi surface, to ensure the final fermion state has zero energy: this places a second constraint on $\vec{k}_2$. The solution of these constraints yields a pair of $(d-2)$-dimensional manifolds specifying the allowed values of $\vec{k}_1$ and

$\vec{k}_2$: these are the "hot" manifolds. In $d = 2$, they become the "hot spots" shown in Fig. III for the cuprate case.

We take the continuum limit by focusing on one generic point on the hot manifold, say $\vec{k}_1$. Then its partner, $\vec{k}_2 = \vec{k}_1 + \vec{K}$ will also be on the hot manifold. We will focus on the patches of the Fermi surface near these points. There are several other pairs of patches in the Brillouin zone, as is clear from Fig. 10: these will be described by parallel theories which we will not discuss explicitly. Within a given pair of Fermi surface patches, our results will not depend upon the specific choices of $\vec{k}_{1,2}$ on the hot manifold: this will be evident from our continuum theory below, and will not require a proof which is the analog of Section I A.

Near $\vec{k}_1$ and $\vec{k}_2$, we define continuum fields $\psi_{1,2}$, as in (48)

$$\psi_{1a}(\vec{k}) = c_{\vec{k}_1+\vec{k},a} \quad , \quad \psi_{2a}(\vec{k}) = c_{\vec{k}_2+\vec{k},a}. \tag{61}$$

We insert this into (1) and expand in powers of k. Unlike the situation in Sections I and II, it will turn out here that it is sufficient to keep terms only linear in k, and

the analog of (7) is

$$\mathcal{S}_\psi = \int d\tau \int d^d x \left[\psi_{1a}^\dagger \left(\zeta \frac{\partial}{\partial \tau} - i \vec{v}_1 \cdot \nabla_x \right) \psi_{1a} + \psi_{2a}^\dagger \left(\zeta \frac{\partial}{\partial \tau} - i \vec{v}_2 \cdot \nabla_x \right) \psi_{2a} \right]. \quad (62)$$

Here $\vec{v}_1 = \nabla_k \varepsilon_k|_{k_1}$ is the Fermi velocity at $\vec{k}_1$, and similarly for $\vec{v}_2$. We have inserted factors of ζ in front of the temporal derivatives by analogy with Section II B, anticipating that the temporal derivatives will ultimately become irrelevant near the critical point. In the $\psi_{1,2}$ formulation, the configurations of the Fermi surfaces and hot manifolds are shown in Fig. 11. The Fermi surface of the ψ_1 fermions is defined by $\vec{v}_1 \cdot \vec{k} = 0$, and the Fermi surface of the ψ_2 fermions is defined by $\vec{v}_2 \cdot \vec{k} = 0$. Finally, the hot manifold is defined by the $\vec{k}$ which satisfy *both* these conditions. We assume here and below that $\vec{v}_1$ and $\vec{v}_2$ are not collinear: the collinear case corresponds to the "nesting" of the Fermi surfaces, and we do not consider that here.

It is now a simple matter to take the continuum limit of the boson-fermion cou-

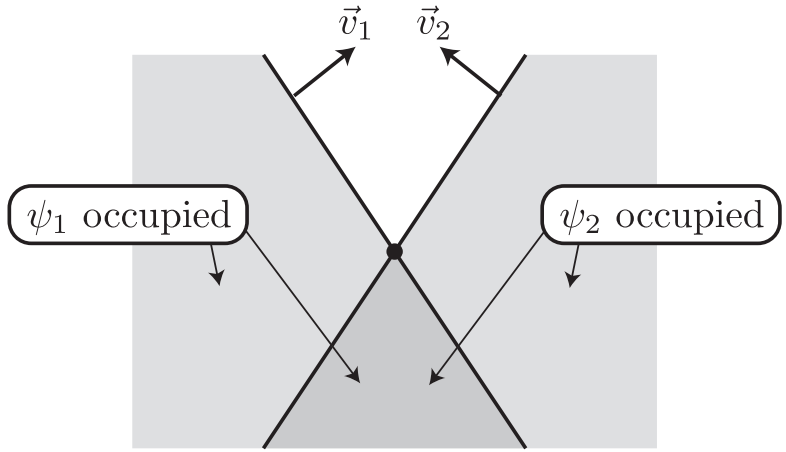

FIG. 11: Fermi surfaces of ψ_1 and ψ_2 fermions in the plane defined by the Fermi velocities $\vec{v}_1$ and $\vec{v}_2$. The Fermi surfaces are $d-1$ dimensional, and are indicated by the full lines. The $d-2$ dimensional "hot manifold" intersects this plane at the filled circle at the origin.

pling in (59). Including the important terms in $\mathcal{S}_\phi$, we obtain

$$\mathcal{S}_{\psi\phi} = \int d^dx \int d\tau \left[\frac{1}{2}(\nabla_x \phi_\alpha)^2 + \frac{r}{2}\phi_\alpha^2 + \frac{u}{4}\left(\phi_\alpha^2\right)^2 + \lambda \phi_\alpha \sigma^\alpha_{ab} \left(\psi^\dagger_{1a}\psi_{2b} + \psi^\dagger_{2a}\psi_{1b} \right) \right]. \tag{63}$$

Here we have omitted the temporal gradient term in ϕ_α because it will later turn

out to be irrelevant.

The remaining analysis of this section will work with the continuum theory of bosons and fermions defined by $\mathcal{S}_\psi + \mathcal{S}_{\psi\phi}$ defined in (62) and (63). Our steps in the following subsection will closely parallel those for the Ising-nematic case in Section II.

We begin by noting the Fermi surface change in the SDW phase of $\mathcal{S}_\psi + \mathcal{S}_{\psi\phi}$. Setting $\phi_\alpha = (0, 0, \phi)$, and diagonalizing the $\psi_{1,2}$ spectrum, it is a simple matter to show that the Fermi surfaces in Fig. 11 and modified to those in Fig. 12.

C. Hertz theory

As in Section II A, the Hertz theory for the SDW order ϕ_α is obtained by integrating out the $\psi_{1,2}$ fermions from $\mathcal{S}_\psi + \mathcal{S}_{\psi\phi}$ in (62) and (63).

Again, the most important contribution is the co-efficient of the ϕ_α^2 term, which is given by the fermion polarizability in Fig. 7. Here the explicit expression for the polarizability maps from (17) to

$$\Pi(q, \omega_n) = \int \frac{d^d k}{(2\pi)^d} \int \frac{d\epsilon_n}{2\pi} \frac{1}{[-i\zeta(\epsilon_n + \omega_n) + \vec{v}_1 \cdot (\vec{k} + \vec{q})][-i\zeta\epsilon_n + \vec{v}_2 \cdot \vec{k}]}. \quad (64)$$

We define oblique co-ordinates $p_1 = \vec{v}_1 \cdot \vec{k}$ and $p_2 = \vec{v}_2 \cdot \vec{k}$. It is then clear that the

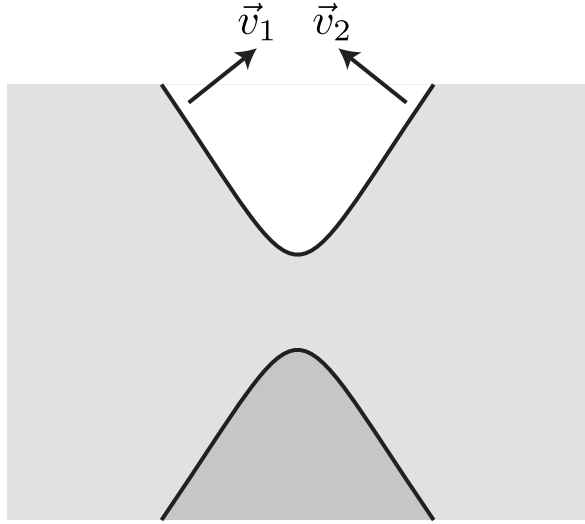

FIG. 12: Modification of the Fermi surfaces in Fig. 11 by SDW order with $\langle \phi_\alpha \rangle \neq 0$. The full lines are the Fermi surfaces, and the white, light shaded, and dark shaded regions denote momenta where 0, 1, and 2 of the bands in (60) are occupied. The upper and lower lines are boundaries of hole and electron pockets respectively. There are 8 instances of such Fermi surface configurations in Fig. 10c, centered on the 8 hotspots.

integrand in (64) is independent of the $(d-2)$ transverse momenta, whose integral yields an overall factor Λ^{d-2} (in $d=2$ this factor is precisely 1). Also, by shifting the integral over k_1 we note that the integral is independent of q. So we have

$$\Pi(q,\omega_n) = \frac{\Lambda^{d-2}}{|\vec{v}_1 \times \vec{v}_2|} \int \frac{dp_1 dp_2 d\epsilon_n}{8\pi^3} \frac{1}{[-i\zeta(\epsilon_n+\omega_n)+p_1][-i\zeta\epsilon_n+p_2]}. \tag{65}$$

Next, we evaluate the frequency integral to obtain

$$\begin{aligned}\Pi(q,\omega_n) &= \frac{\Lambda^{d-2}}{\zeta|\vec{v}_1\times\vec{v}_2|}\int\frac{dp_1dp_2}{4\pi^2}\frac{[\mathrm{sgn}(p_2)-\mathrm{sgn}(p_1)]}{-i\zeta\omega_n+p_1-p_2}\\ &= -\frac{|\omega_n|\Lambda^{d-2}}{4\pi|\vec{v}_1\times\vec{v}_2|}.\end{aligned} \tag{66}$$

In the last step, we have dropped a frequency-independent, cutoff-dependent constant which can absorbed into a redefinition of r. Notice also that the factor of ζ has cancelled.

Inserting this fermion polarizability in the effective action for ϕ_α, we obtain the Hertz action for the SDW transition; here (33) is replaced by

$$\begin{aligned}\mathcal{S}_H = \int\frac{d^dk}{(2\pi)^d}T\sum_{\omega_n}\frac{1}{2}\left[k^2+\gamma|\omega_n|+r\right]|\phi_\alpha(k,\omega_n)|^2\\ +\frac{u}{24}\int d^dxd\tau\left(\phi_\alpha^2(x,\tau)\right)^2.\end{aligned} \tag{67}$$

The main difference from (33) is that the $|\omega_n|/|k|$ has been replaced by a $|\omega_n|$: this is a direct consequence of the Fermi surface structure in Fig. 11, which leads to a density of states of particle-hole excitations which a linear in energy, and independent of momentum.

The subsequent analysis of the above Hertz action proceeds just as in (34) and (35), but now with dynamic exponent $z = 2$. Again, this exponent characterizes the frequency scale $\omega \sim k^2$ emerging from a comparison of the first two terms in (67). Now we see that the Gaussian fixed point of (67) is stable for $d > 2$.

Just as in Section II, we will see below that the Hertz approach is essentially correct in $d = 3$, but that it fails in the physically important case of $d = 2$, and not just by a marginal correction. The key to this will be an examination of the fermion spectrum and the RG flow of the fermion-boson coupling, to which we turn to in Section III D.

D. Fate of the fermions

We proceed just as in Section II B. With the scaling dimensions of spacetime and ϕ as in (34) with $z = 2$, the action $\mathcal{S}_\psi$ in (62) implies the tree level rescaling

$$\dim[\psi] = (d+1)/2 \quad , \quad \dim[\zeta] = -1. \tag{68}$$

Thus, just as in Section II B and II C, ζ is irrelevant, and can eventually be sent to 0. Finally, evaluating the scaling dimension of the λ term in $\mathcal{S}_{\psi\phi}$ in (63), we obtain

the same result as in (41), namely

$$\dim[\lambda] = \frac{(2-d)}{2}. \tag{69}$$

The conclusions then are the same as in Section II B: a perturbative theory in λ, in the Hertz/RPA approach is valid in $d = 3$, but requires a new formulation in terms of a fixed λ theory in $d = 2$.

The remaining analysis in this subsection tracks that below (41) in Section II B.

The perturbative estimate for the fermion damping on the hot manifold is given by (42). Using the values here $\dim[\Sigma] = 1$ and $\dim[\omega] = 2$, we obtain instead of (43) that

$$p = \frac{d-1}{2}. \tag{70}$$

In $d = 3$, this has the same value as in (43), and so the conclusions are the same.

In $d = 2$, we obtain non-Fermi liquid behavior at the hot spots with $\mathrm{Im}\Sigma \sim \sqrt{\omega}$.

We verify this result by explicitly computing the value of the fermion damping from the graph in Fig. 8. At zero momentum for the ψ_1 fermion we have, instead of (45)

$$\Sigma_1(0,\omega_n) = \lambda^2 \int \frac{d^d q}{(2\pi)^d} \int \frac{d\epsilon_n}{2\pi} \frac{1}{[q^2 + \gamma|\epsilon_n|\,]\,[-i\zeta(\epsilon_n+\omega_n) + \vec{v}_2\cdot\vec{q}\,]}. \tag{71}$$

We first perform the integral over the $\vec{q}$ direction parallel to $\vec{v}_2$, while ignoring the subdominant dependence on this momentum in the boson propagator. The dependence on ζ immediately disappears, and yields in place of (46),

$$\Sigma_1(0,\omega_n) = i\,\frac{\lambda^2}{|v_2|}\int\frac{d^{d-1}q}{(2\pi)^{d-1}}\int\frac{d\epsilon_n}{2\pi}\frac{\mathrm{sgn}(\epsilon_n+\omega_n)}{|q|^2+\gamma|\epsilon_n|}$$
$$= i\,\frac{\lambda^2}{\pi|v_2|\gamma}\mathrm{sgn}(\omega_n)\int\frac{d^{d-1}q}{(2\pi)^{d-1}}\ln\left(\frac{|q|^2+\gamma|\omega_n|}{|q|^2}\right). \qquad (72)$$

Again, evaluation of the q integral yields results in agreement with the scaling estimate (70). Specifically, in $d=2$, (72) evaluates to

$$\Sigma_1(0,\omega) = i\,\frac{\lambda^2}{\pi|v_2|\sqrt{\gamma}}\mathrm{sgn}(\omega_n)\sqrt{|\omega_n|} \quad , \quad d=2, \qquad (73)$$

as expected from (70).

E. Critical theory in $d = 2$

With the conclusion of Section III D that the Hertz theory only applies for $d = 3$, let us turn to the strong coupling dynamics in $d = 2$. Following Section II C, we need

to understand the renormalization structure of the underlying theory of fermions and bosons, without an integration of the fermionic modes.

In the present case, the needed critical theory in $d = 2$ was already formulated in Section III B. It is defined by $\mathcal{S}_\psi + \mathcal{S}_{\psi\phi}$ in (62) and (63).

We formulate the RG with the same spacetime rescalings used in Section III C:

$$\dim[x] = -1 \quad , \quad \dim[\tau] = -2. \tag{74}$$

Note that we do not allow an anomalous dimension in the rescaling of τ. This does not mean that we necessarily have dynamic exponent $z = 2$. We will allow the Fermi velocities $\vec{v}_1$ and $\vec{v}_2$ to flow under the RG, and a non-trivial z will arise from the nature of their flow to large scales. It is convenient to use such a formulation because the scaling of the fermion spectrum depends sensitively on the direction in momentum space, and the shape of the Fermi surface also evolves.

We do, however, have to allow for anomalous dimensions in the field rescalings, which become

$$\dim[\phi] = (2 + \eta_\phi)/2 \quad , \quad \dim[\psi] = (3 + \eta_\psi)/2 \tag{75}$$

Contributions to these anomalous dimensions do arise from loop fluctuation contributions.

Next, as in (55), we have the tree-level rescalings of the couplings associated with

the fermions:

$$\dim[\zeta] = -1 - \eta_\psi \quad , \quad \dim[\lambda] = -(\eta_\phi + 2\eta_\psi)/2. \tag{76}$$

We reach the same conclusions from these results that we did in Section II C. We can safely assume that $\zeta = 0^+$, and use this value in loop computations. With the absence of the ζ term, we can choose the fermion field scale renormalization so that the theory maintains $\lambda = 1$. So there is a strong fermion-boson coupling at all scales, and no independent renormalization group flow for λ.

The task before us is now clear, in principle. We have to evaluate higher loop diagrams and so determine the RG flow of the couplings $\vec{v}_1$, $\vec{v}_2$, r, and u, and the anomalous dimensions η_ϕ and η_ψ. Note that the boson damping co-efficient γ in the Hertz action (67) does *not* appear as an independent coupling. In reality, it is a parameter in the boson spectral function, and its value is pinned to the underlying couplings via (66); it is reassuring that the value in (66) has no non-universal cutoff dependence in $d = 2$.

The evaluation of these higher loop diagrams is very involved, and the reader is referred to Refs. [11–14] for further details. These papers describe the rather complex structure of the dynamic response of the fermions and the bosons near the quantum critical point. Here we focus on just one striking aspect: the shape of the Fermi surface. This is determined by the flow of the velocities near the critical

point. Let us write the velocities as

$$\vec{v}_1 = (v_x, v_y) \quad , \quad \vec{v}_2 = (-v_x, v_y). \tag{77}$$

Then to two-loop order, the RG flow of the velocity ratio is given by

$$\frac{d\alpha}{d\ell} = -\frac{12}{\pi n}\frac{\alpha^2}{\alpha^2+1} \quad , \quad \alpha \equiv \frac{v_y}{v_x} \tag{78}$$

in a model with n pairs of hot spots (the Fermi surface in Fig. 10 has $n = 4$). Integrating (78), we observe that α scales logarithmically to zero with momentum scale. We can use the distance from the hot spot to set the momentum scale. The location of the ψ_1 Fermi surface is given by $\vec{v}_1 \cdot \vec{k} = 0$, or $k_y = -v_x k_x / v_y = -k_x/\alpha$. Evaluating α at the scale k_x, we find the Fermi surfaces of the $\psi_{1,2}$ at

$$k_y = \pm \frac{12}{\pi n} k_x \log(1/|k_x|). \tag{79}$$

Such Fermi surfaces are sketched in Fig 13

---

[1] Hertz, J. A. (1976) *Phys. Rev. B* **14**, 1165.

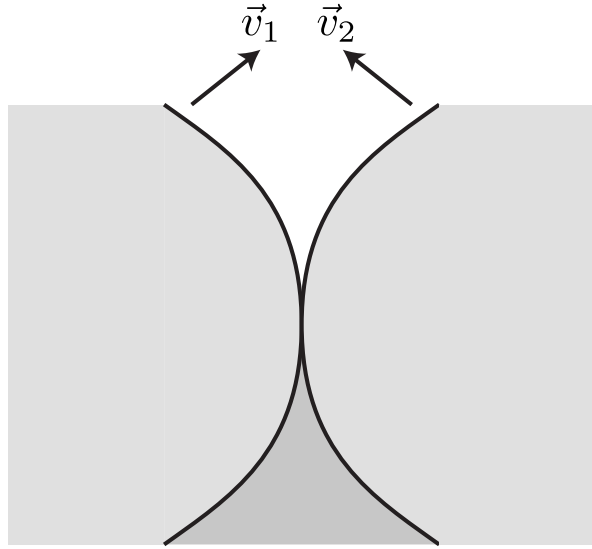

FIG. 13: Modification of the Fermi surfaces in Fig. 11 at the SDW quantum critical point. As in Figs. 11 and 12, the full lines are the Fermi surfaces, and the white, light shaded, and dark shaded regions denote momenta where 0, 1, and 2 of the bands in (60) are occupied. The equations of the Fermi surfaces are given in (79).

[2] Beal-Monod, M. T., and Maki, K. (1975) *Phys. Rev. Lett.* **34**, 1461.
[3] Moriya, T., and Kawabata, A. (1973) *J. Phys. Soc. Jpn.* **34**, 639.
[4] Moriya, T., and Kawabata, A. (1973) *J. Phys. Soc. Jpn.* **35**, 669.
[5] Ramakrishnan, T. V. (1974) *Phys. Rev. B* **10**, 4014.
[6] Shankar, R. (1994) *Rev. Mod. Phys.* **66**, 129.
[7] Metlitski, M., and Sachdev, S. (2010), arXiv:1001.1153.
[8] Varma, C. M., Littlewood, P. B., Schmitt-Rink, S., Abrahams, E., and Rucken-

stein, A. E. (1989) *Phys. Rev. Lett.* **63**, 1996.
[9] Lee, S. S. (2009) *Phys. Rev. B* **80**, 165102.
[10] Sachdev, S., Chubukov, A. V., and Sokol, A. (1995) *Phys. Rev. B* **51**, 14874.
[11] Abanov, Ar., and Chubukov, A. (2000) *Phys. Rev. Lett.* **84**, 5608.
[12] Abanov, Ar., and Chubukov, A. (2004) *Phys. Rev. Lett.* **93**, 255702.
[13] Abanov, Ar., and Chubukov, A., and Schmalian, J. (2003) *Advances in Physics* **52**, 119.
[14] Metlitski, M., and Sachdev, S. (2010), arXiv:1005.1288.